

Numerical analysis of non-resonant mode in LHD partial collapse with net toroidal current

メタデータ	<p>言語: eng</p> <p>出版者:</p> <p>公開日: 2022-07-26</p> <p>キーワード (Ja):</p> <p>キーワード (En):</p> <p>作成者: ICHIGUCHI, Katsuji, SUZUKI, Yasuhiro, TODO, Yasushi, SAKAKIBARA, Satoru, IDA, Katsumi, TAKEMURA, Yuki, SATO, Masahiko, OHDACHI, Satoshi, NARUSHIMA, Yoshiro, SUGIYAMA, L., CARRERAS, Benjamin A.</p> <p>メールアドレス:</p> <p>所属:</p>
URL	http://hdl.handle.net/10655/00013413

This work is licensed under a Creative Commons Attribution 3.0 International License.



Numerical analysis of non-resonant mode in LHD partial collapse with net toroidal current

K. Ichiguchi^{1,2}, Y. Suzuki^{1,2}, Y. Todo¹, S. Sakakibara^{1,2}, K. Ida^{1,2}, Y. Takemura^{1,2}, M. Sato¹,
S. Ohdachi¹, Y. Narushima^{1,2}, L. E. Sugiyama³ and B. A. Carreras⁴

¹*National Institute for Fusion Science, Oroshi-cho 322-6, Toki 509-5292, Japan*

²*The Graduate University for Advanced Studies, SOKENDAI, Toki, 509-5292, Japan*

³*Massachusetts Institute of Technology, Cambridge MA 02139-4307, USA*

⁴*BACV Solutions Inc., Oak Ridge, Tennessee 37831, USA*

1. Introduction

The global stability of the plasma in the Large Helical Device (LHD) is extensively studied in the experiments. In the experiments, partial collapse phenomena are observed when the net toroidal current is driven by the neutral beam injection so that the rotational transform ι is increased[1]. These collapses are always caused by the $(m, n) = (1, 1)$ mode. Here, m and n are the poloidal and the toroidal mode numbers, respectively. This mode is considered to be a pressure driven mode because the equilibria are strongly Mercier unstable. However, according to the theory of pressure driven modes, the linear growth rate is larger for higher mode numbers. Therefore, it has been required to explain why the partial collapses are caused by the mode with such low mode numbers in LHD. In order to consider the reason, we carry out three-dimensional nonlinear magnetohydrodynamic (MHD) simulations.

2. Numerical calculation

In this simulation, the HINT[2] and the MIPS[3] codes are utilized for the equilibrium and the non-linear dynamics calculations, respectively. In the equilibrium calculation, we employ the same vacuum magnetic configuration as shown in Ref.[1]. The equilibrium pressure profile is given by $P_{eq} = P_0 (1 - 0.68\rho^2 - 0.32\rho^4)$ with the axis beta value $\beta_0 = 1.4\%$. The net toroidal current profile is given by $J_{eq} = J_0(1 - \rho^2)^4$ with the total current $I/B = 30\text{kA/T}$. Here, ρ and B denote the normalized

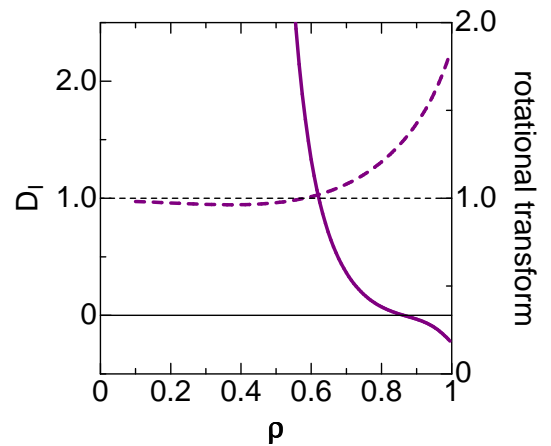


Figure 1: Profiles of Mercier index D_I (solid line) and rotational transform (dashed line) for the $\beta_0 = 1.4\%$ and $I/B = 30\text{kA/T}$ equilibrium.

toroidal flux and the magnetic field strength, respectively. Figure 1 shows the rotational transform and the Mercier index D_I of this equilibrium. The magnetic shear is very low and the rotational transform is close to unity in the core region. At the $\iota = 1$ surface, D_I is significantly large. It is followed that this equilibrium is unstable against the interchange mode resonant at this surface.

Figure 2 shows the time evolution of the total kinetic energy. Here the toroidal component of the kinetic energy for each mode number n is also plotted. The perturbation grows linearly first, then, is saturated. The dominant component in the linear phase is the $n = 3$ component, and the $n = 2$ component is secondary dominant.

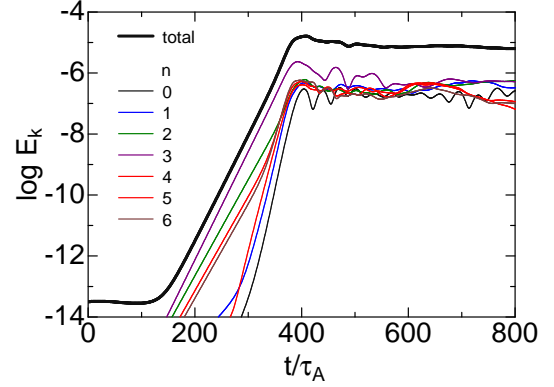


Figure 2: Time evolution of the total kinetic energy E_k (black solid line) and Fourier components of the kinetic energy E_{kn} (thin lines).

Figure 3 shows the absolute value of the Fourier component of the pressure perturbation $|P_{mn}|$, the puncture plots of the field lines and the pattern of the pressure perturbation, and the birds eye view of the total pressure in the typical three timings. At $t = 360\tau_A$, the (3,3) component is dominant as shown in Fig.3(a), where τ_A denotes the Alfvén time. The profile is Gaussian-like, which is localized around the $\iota = 1$ resonant surface. This feature indicates that this mode is a typical interchange mode. Thus, the $m = 3$ perturbation pattern appears as shown in Fig.3(b). The magnetic surfaces and the total pressure deform corresponding to this pattern as shown in Fig.3(b) and (c).

At $t = 480\tau_A$, the (2,2) component becomes dominant. This component is localized in the low shear region which is more inward rather than the resonant surface as shown in Fig. 3(d). In this point of view, this mode is considered as a non-resonant mode. The deformation of the magnetic surfaces and the total pressure shows the $m = 2$ structure as shown in Fig.3(e) and (f).

In addition, at $t = 700\tau_A$, the (1,1) component becomes dominant as shown in Fig.3(g). The profile is also localized in the low shear region and shows a non-resonant structure. The corresponding shapes are seen in the magnetic surfaces and the total pressure as shown in Fig.3(h) and (i). Therefore, as a total, the transition from the (3,3) interchange mode to the (1,1) non-resonant mode is observed in this nonlinear evolution. In this nonlinear transition, the mode number of the dominant component is decreased continuously like an inverse cascade as shown in Fig.4. Similar results are obtained in the case of $I/B = 29.6\text{kA/T}$ [4]. However, the superiority of the (1,1) component to others after the transition is more remarkable in the case of

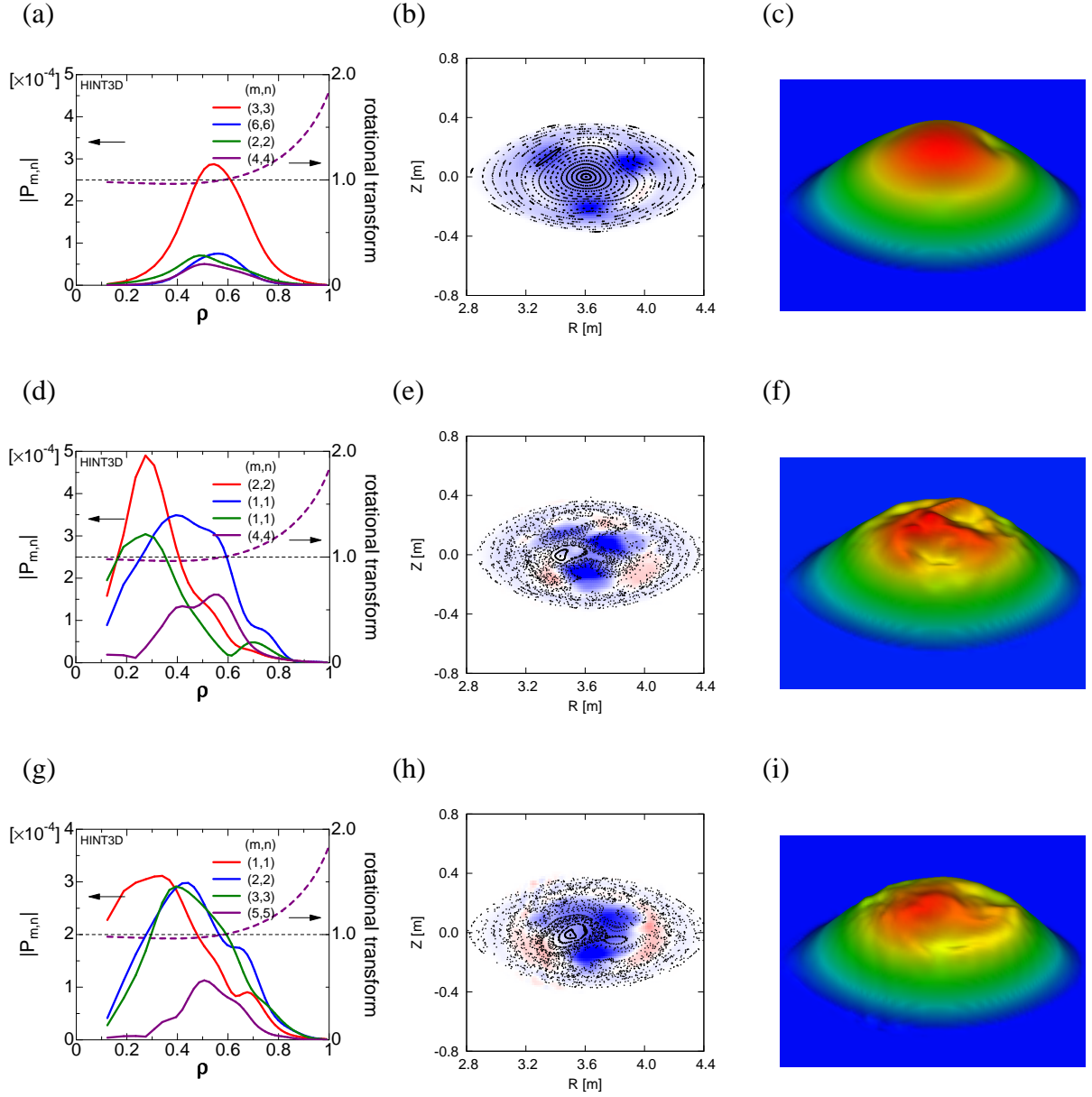


Figure 3: (a), (d) and (g) profiles of the largest four Fourier components of the perturbed pressure absolute value, (b), (e) and (h) pattern of the perturbed pressure and the puncture plots of the field lines and (c), (f) and (i) bird's eye view of the total pressure at (a)-(c) $t = 360\tau_A$, (d)-(f) $t = 480\tau_A$ and (g)-(i) $t = 700\tau_A$ for $I/B = 30\text{kA/T}$ and $\beta_0 = 1.4\%$. Thick dashed line shows the profile of the equilibrium rotational transform in (a), (d) and (g).

$$I/B = 29.6 \text{ kA/T.}$$

3. Summary

We have found the transition from the (3,3) interchange mode to the (1,1) non-resonant mode. This transition occurs in the case that the rotational transform has a low shear in the core region and has the value close to unity in the region. This profile is generated by the net toroidal current in the present study. On the other hand, in the no net toroidal current with a high shear case, a typical interchange mode with higher mode number is destabilized[4]. In this case, several components with comparable amplitude appear simultaneously in the nonlinear evolution. The pressure structure becomes quite

complicated. Thus, the transition to a non-resonant mode does not occur. From this difference, the condition that the low shear rotational transform close to unity is considered to be necessary for such a transition. In the LHD experiments, the partial collapses are caused by the (1,1) mode. Thus, this transition can be one of the candidate to explain the mode number observed in the experiments. On the other hand, the difference from $I/B = 29.6 \text{ kA/T}$ is also obtained. Precise analysis for the total current dependence of the transition will be necessary in future.

Acknowledgments

This work was performed on "Plasma Simulator" (NEC SX-Aurora TSUBASA) of National Institute for Fusion Science (NIFS) with the support and under the auspices of the NIFS Collaboration Research program (NIFS20KNST159) and on the JFRS-1 supercomputer system at Computational Simulation Centre of International Fusion Energy Research Centre (IFERC-CSC) in Rokkasho Fusion Institute of QST (Aomori, Japan). This work was partly supported by KAKENHI (15K06651, 20K03909) by Japan Society for the Promotion of Science (JSPS).

References

- [1] S. Sakakibara, et al., Nucl. Fusion, **55**, 083020 (2015).
- [2] Y. Suzuki, et al, Nucl. Fusion **46** (2006) L19.
- [3] Y. Todo, et al, Plasma and Fusion Res. **5** (2010) S2062.
- [4] K. Ichiguchi, et al, submitted to Nucl. Fusion.

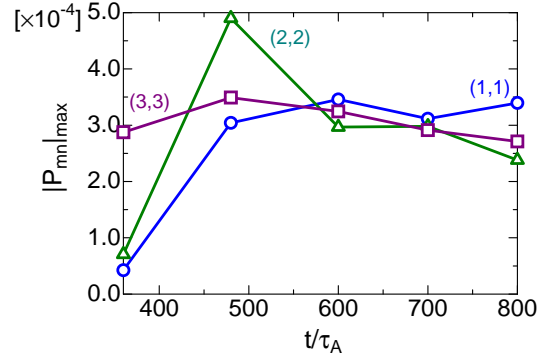


Figure 4: Time evolution of the maximum value of $|P_{mn}|$ for $(m,n) = (1,1)$, $(2,2)$, and $(3,3)$.